Back contact nature effect on the CZTS/ZnS based heterojunction

S. Mahjoubi [a], N. Bitri [a], E. Aubry [b], F. Chaabouni [a] and P. Briois [b]

[a] Université de Tunis El Manar, Ecole Nationale d'Ingénieurs de Tunis, Laboratoire de Photovoltaïque et Matériaux semi-conducteurs, 1002 Tunis, Tunisie
[b] Institut FEMTO-ST, UMR 6174, CNRS, UTBM, Univ. Bourgogne Franche-Comté, Site de Montbéliard, 90010 Belfort, France

Abstract

This work contributes to the discussion on the influence of the back contact on the electrical properties of Cu_2ZnSnS_4 (CZTS) based solar cells. Devices with noble metals back contact (Au, Ag and Pt) such as FTO/ZnS/CZTS/Au, FTO/ZnS/CZTS/Pt and FTO/ZnS/CZTS/Ag were investigated by means of the current voltage characteristic in the dark (FTO = fluorine-doped tin oxide). The originality of this work is that all active layers (absorbing and buffer layers) are deposited by the same system using spray pyrolysis technique. The metallic back contacts are sputter deposited. X-ray diffraction (XRD) and UV-visible spectrophotometry were used to investigate the main structural and optical properties of different layers constituting the solar cell. The electrical characterization achieved by I-V characteristic proves that all synthesized heterojunctions exhibit a rectifying behavior. Furthermore, the ideality factors of Au, Pt and Ag back contacts were estimated to 1.6, 2.4 and 2.8, respectively. The lower saturation current and series resistance are measured in the heterojunction using Au as a back contact. From this study, it is shown that Au back contact could be an alternative of Mo in CZTS based solar cell prepared by spray pyrolysis.

Keywords: Thin films, Spray, Cu_2ZnSnS_4, Back contact, Heterojunction, solar cells.

Introduction

Cu_2ZnSnS_4 (CZTS) thin films is considered to be a promising candidate for low cost and high efficiency thin film solar cells with record device efficiencies of about 12 % **[1].**

The elements of CZTS thin films is abundant in the earth crust, non-toxic and encouraging photovoltaic device performances Contrary to CdTe and CIGS absorbing layer, CZTS is a quaternary compound having p-type semiconductor behaviour with the kesterite crystal structure space group I-42m. It shows a relatively high absorption coefficient higher than 10^4 cm^{-1} and a direct band gap in the range of 1.4-1.5 eV **[2,3,4].** These features make it a highly suitable material as an absorber thin film for low-cost thin film solar cells.

In addition to its application in conventional thin film solar cells, CZTS is widely used in others application such as gas sensor and photocatalytic **[5, 6, 7].** Yuting Wang et al **[5]** have

1

synthesized a Cu_2ZnSnS_4 (CZTS)-based gas sensor incorporated by polyoxometalate (POMs) electron acceptor by hydrothermal method. They confirm that the incorporation of POMs can form a shallow electronic trap, accelerate the electron transfer and enhance the performance of CZTS. Gurav et al [6] have invesigated the sensing liquefied petroleum gas (LPG) properties of p-CZTS/n-ZnO heterojunction.

Sampath et al have [7] studied the structural, optical and photocatalytic properties of spray deposited Cu_2ZnSnS_4 thin films with various S/(Cu+Zn+Sn) ratio. They founded that the presence of secondary phase significantly affects the photocatalytic performance of CZTS thin films.

In the literature, the structure of the solar cell based CZTS is directly copied from those used in $Cu(In,Ga)Se_2$ (CIGS) technology such as p-type absorber (CZTS) and n-type buffer (ZnS) thin films constituting the heterojunction inserted between two electrodes.

CdS thin film is the most buffer layer used in CZTS solar cells [8, 9]. However, the toxicity, high cost of cadmium and its relative narrow band gap (around 2.41 eV) [10, 11] are considered obstacles for solar cells application.

For this reason, new semiconductors are studied to replace CdS. Among them, ZnS has attracted great attention as a promising buffer layer for solar cells owing to its tunable and direct band gap (3.65 eV) and earth-abundant elements [12,13].

Numerous studies done on the electrical properties of the back contact in solar cells have shown that they strongly influence the solar cell performances. Mo film is the commonly used back contact. However, Mo back contact may be due to the formation of MoS_2 at the interface. Mo/CZTS back contact is associated to a MoS_2 layer behaving as a blocking back contact.

Indeed Scragg et al. [14] recommended reexamining the choice of molybdenum at CZTSSe|Mo. Patel and Ray [15] numerically simulated the current-voltage (I-V) characteristics of a Al:ZnO/i-ZnO/CdS/CZTSSe/BC solar cell trying to find the optimum BC (back contact) which would give the best cell performances. In this context, three different metals (Au, Pt and Ag) are tested as back contact instead of commonly used Mo.

In this work, the effect of the nature of the metal back contact on the electrical properties of CZTS/ZnS based heterojunction prepared by spray pyrolysis is studied and the originality of this work is that all active layers (absorbing and buffer layers) are deposited by the same system using spray pyrolysis technique.

Experimental details

Preparation and deposition of CZTS thin film, ZnS buffer layer and FTO transparent front contact layer.

FTO coated on glass substrates is used as transparent front contact layer. It admits a sheet resistance in the range of 6-8 Ω square and has a thickness of about 500 nm.

The ZnS buffer layer has been grown on FTO substrates using chemical spray technique at 400°C for 30 min. The solution for ZnS layer was prepared from a solution composed with a mixture of Zinc chloride hexahydrate $ZnCl_2$(6 H_2O) (0.1 M) and of thiourea $SC(NH_2)_2$ (0.05 M) and has a thickness of 100 nm. The Cu_2ZnSnS_4 absorbing layer has been synthesized with the chemical spray process using the "Spray Sandwich" technique consisting in the deposition of three successively layers: $ZnS/SnS_2/Cu_2S$. The starting solutions were composed of zinc chloride hexahydrate $ZnCl_2$(6 H_2O) (0.01 M), tin chloride dihydrate $SnCl_2$(2 H_2O) (0.01 M), copper chloride dihydrate $CuCl_2$(2 H_2O) (0.04 M), mixed respectively with thiourea $SC(NH_2)_2$ (0.01 M) as chemical precursors. The CZTS thin films were obtained by spraying three solutions, starting by the deposition of the solution containing a ZnS, the following solution contains a $SnS2$ and the last solution contains $Cu2S$ respectively at 420°C, 400°C and 300°C of the substrate temperature. The solutions were sprayed at the rate of 2ml/min.

 All chemicals were purchased from Sigma-Aldrich. The CZTS thin film has a thickness of 800 nm. The scheme of the heterostructure and cross-sectional micrograph of the solar cell based CZTS are given in Fig.1.

Three metals are tested as back contact namely gold (Au), platinum (Pt) and silver (Ag). All back contacts were deposited by direct current magnetron sputtering. Three different contacts (Pt, Ag, and Au) using masks are deposited successively of the top surface of the device (as shown in figure 1) in order to have the same heterojunction. The metallic coatings have been deposited by sputtering of metallic targets in pure argon atmosphere. Pulsed DC supplies powered the platinum (Pt, purity 99.95%), or silver (Ag, purity 99.5%) or gold (Au, purity 9.95%) targets mounted on balanced magnetrons, respectively an Advanced Energy Pinacle+ pulsed at a fix frequency of 100 kHz. The reactor was a 90-litre cylinder pumped down with a turbo molecular pumping system allowing a base vacuum of less than 10^{-4} Pa before refilling with argon at the convenient pressure. The argon flow rate introduced in the deposition chamber was controlled by a Brooks flowmeter and his value is fixed at 50 sccm. In this condition, the total pressure was 0.5 Pa and was measured using a MKS Baratron Gauge.

The targets, 50 mm in diameter and 3 mm in thickness, are parallel to the substrate-holder and are spaced by 120 mm from each other. Their distance from the substrate holder (DT-S) has been fixed at 60 mm. During the deposition stage, the different substrates have been regularly rotated (20 RPM). The Pt, Au discharge current has been fixed at 0.2 A and 0.1A for Ag target. The deposition time was 2 minutes for all coatings.

Characterization methods

The thickness of the layers has been determined by modelling the transmittance spectra of the translucent metallic coatings deposited on glass substrate (Scout software) [16]. The total transmittance was measured by spectrophotometry with a Shimadzu UV-3600 spectrometer equipped with ISR-3100 integrating sphere (220-2600 nm), standard white board was used for the baseline. It has to be noticed that no effective medium approximations were necessary to obtain a satisfying model (deviation less than $4\ 10^{-4}$) meaning that the metallic coatings were relatively smooth with a good surface coverage. The thicknesses of the Ag, Au and Pt layers are estimated at 50 ± 2 nm, 35 ± 1 nm and 50 ± 1 nm, respectively.

In order to characterize the physical properties of the prepared layers, the layers were also sprayed on the glass substrates. The structure of the films was examined by high-resolution X-ray diffraction (XRD, X'pert PRO, Philips) with monochromatic CuKα radiation ($\lambda = 1.541874$ Å) at 40 kV and 30 mA in θ-2θ configuration from 10 to 70° with a step of 0.05°. UV–Vis spectrophotometer (Shimadzu UV 3100S) were studied to ascertain the transmittance and reflectance measurements for determining the optical parameters such as the absorption coefficient and the optical band gap energy. The optical absorption coefficient (α) is evaluated from the transmittance (T) and reflectance (R) measurements using the following relation:

$$\alpha = \left(\frac{1}{d}\right) \times \ln\left(\frac{(1 - R)^2}{T}\right)$$

The optical band gaps are estimated from the extrapolation of linear region of the plots of $(\alpha h\nu)^2$ versus hν curves. the optical band gap energy (Eg) is obtained according to the Tauc's relation
$\alpha h\nu = A(h\nu - Eg)^n$

where α is the absorption in semiconductor, hυ is photon energy, Eg offered the bandgap energy, n depends on the transition probability, it takes the value of ½ or 2 correspondings to indirect and direct bandgaps, respectively

The electrical properties were studied using current voltage (I-V) characteristic in the dark with a sourcemeter Keithley 2400.
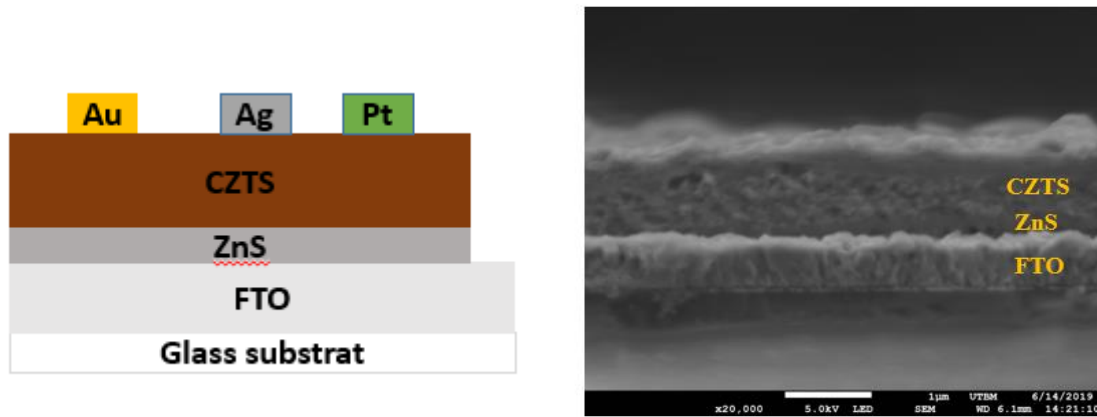

Fig.1 Heterostructure and cross-sectional of the solar cell based CZTS

Results and discussion

FTO film properties

The X-ray diffractogram of the FTO (SnO_2:F) is shown in Fig.2. Main peaks were observed at 26.7°, 33.9°, 37.9°, 51.6°,54.7°, 61.7° and 65.6°which are respectively assigned to (110), (101), (200), (211), (220), (310) and (301) planes of the tetragonal system related to the tin oxide (P42/mnm). This confirms the presence of the SnO_2 material and its relatively good cristallization with (110) as preferential orientation. This result is in good agreement with previous studies which used the spray pyrolysis and sol gel method to deposit the FTO layer **[17, 18].**
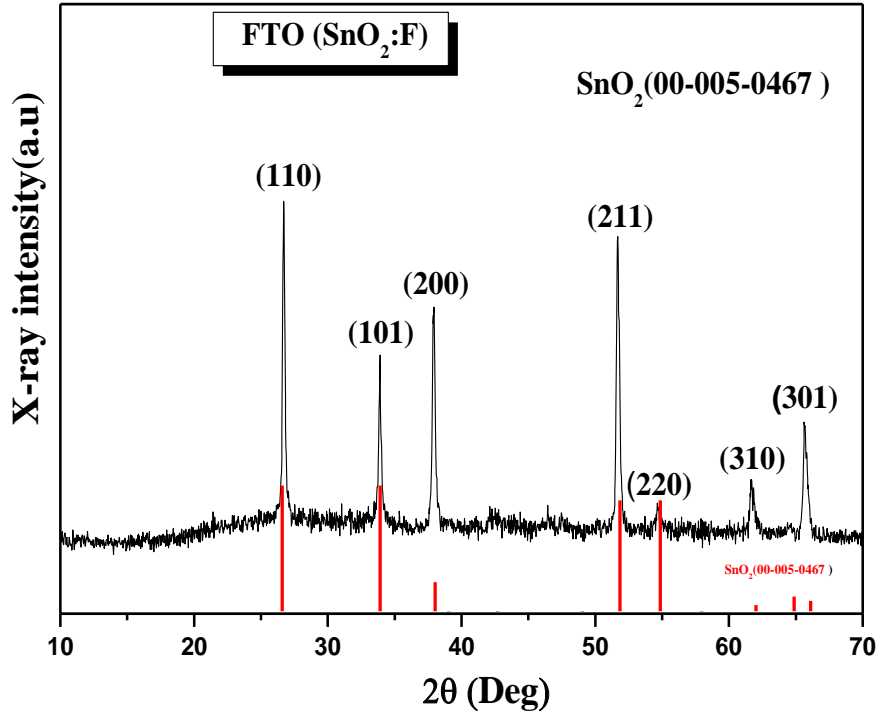
Fig.2 X-ray diffractogram of FTO thin film

Optical properties of FTO film used in the heterojunction structure were studied using UV-visible spectrophotometry in 300 to 1800 nm wavelength range. Transmittance spectrum and Tauc plot of FTO thin films are given in Figure 3 (a-b). The FTO layer exhibits a large transmittance value of about 70-80 % from the visible to the near infrared (< 1200 nm) regions (Fig 3a). The reduction in the transmittance in the near infrared range ($\lambda > 1200$ nm) is ascribed to intraband transitions by free charge carrier resulting from the incorporation effect of fluorine as a donor into the SnO_2 semiconductor. The light absorption being directly proportional to the free charge carrier, the loss of transmittance from 70-80 to 10-20 % shows the relatively high concentration in free electrons in FTO coatings ensuring its electrical conductivity. Using the transmittance spectrum, the optical bandgap energy can be found following the classic Tauc relation [26]

$$\alpha h\nu = A \left(h\nu - E_g \right)^n$$

where α is the coefficient of absorption in cm^{-1}, A is a constant, $h\nu$ the incident photon energy in eV and n is a coefficient corresponding to allowed transition ($= \frac{1}{2}$ for direct transition). Figure 3 (b) shows the plot of $(\alpha h\nu)^2$ vs $h\nu$ and the extrapolation of the linear portion to the $h\nu$-axis to get optical band gap energy. This value for the sprayed FTO film is 3.8 eV. This energy of band gap is consistent with literature [19, 20].
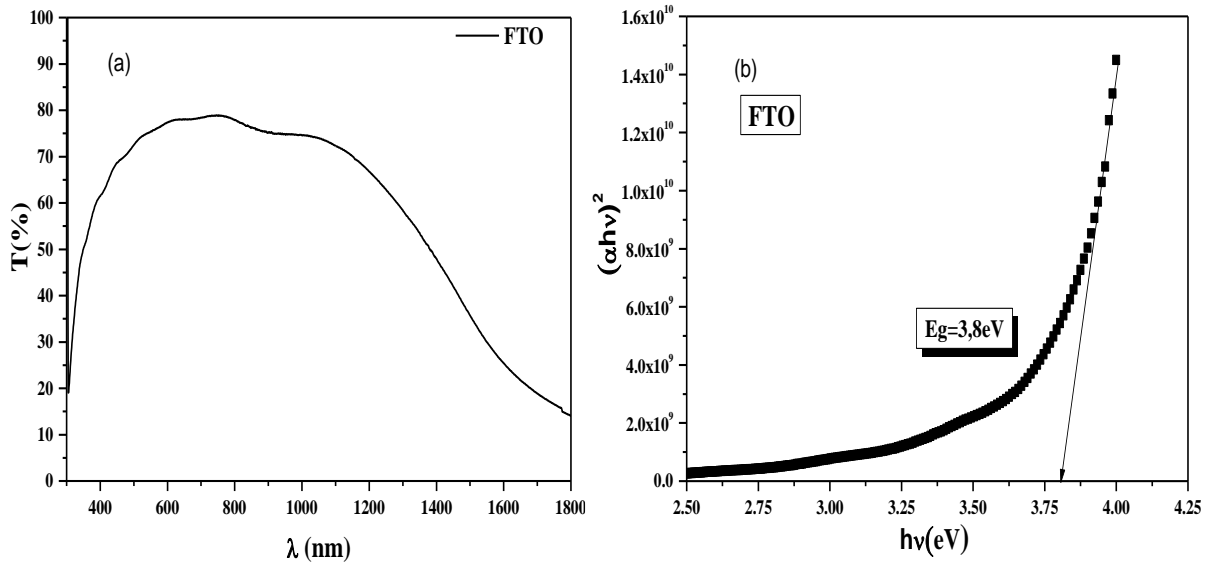
Fig.3 Optical transmittance spectrum (a) and Tauc plot of $(\alpha h v)^2$ versus photon energy (hv) (b) of FTO thin film.

ZnS buffer layer properties

Fig. 4 shows the X-ray diffractogram of the ZnS thin film deposited on glass substrate. The ZnS film crystallizes in both cubic and hexagonal structures. The hexagonal structure is marked by the presence of diffraction lines at 11.31° and 46.48°, which are assigned to (0007) and (1023) planes according to the JCPDS file (83-2336) with a space group P3m1. The cubic phase is observed by the presence of diffraction lines at 28.46° and 47.55° corresponding to the (111) and (220) planes of the cubic phase, respectively (JCPDS Card no. 05-0566) with a space group F-43m. Furthermore, in addition to the ZnS phases, the presence of ZnO phase is noticed. As shown in Fig. 4, the plane (101) of hexagonal wurtzite ZnO structure is clearly visible. This is related to the fact that the preparation of the layers by spray is done in air and in aqueous solution which do not sufficiently prevent from the oxidation of the as-grown layer [21].

The ZnS film exhibits a medium transmittance value in the visible (~ 30-35 %) and a relatively high transparency (> 80 %) in the near infrared region for wavelength higher than 1400 nm (figure 5a). From the transmittance spectrum, the optical band gap energy of the ZnS thin film has been estimated using the Tauc plot method. The band gap energy value is 3.3 eV (Figure 5b).

ZnS film deposited has a band gap equal to 3.34eV, which is narrower than ZnS pure. This gap value has been found by several authors [22,23] and who have shown that: more the temperature

of the substrate increase, more the gap energy is lower than of pure ZnS **[23].** ZnO thin film has a gap energy of around 3.2eV **[24].** Thus, more the layer interacts with oxygen, there is a formation of the ZnO phase and the energy of the gap is lower than of pure ZnS. This may explain the presence of the ZnO phase in the X-ray diffraction spectrum obtained.
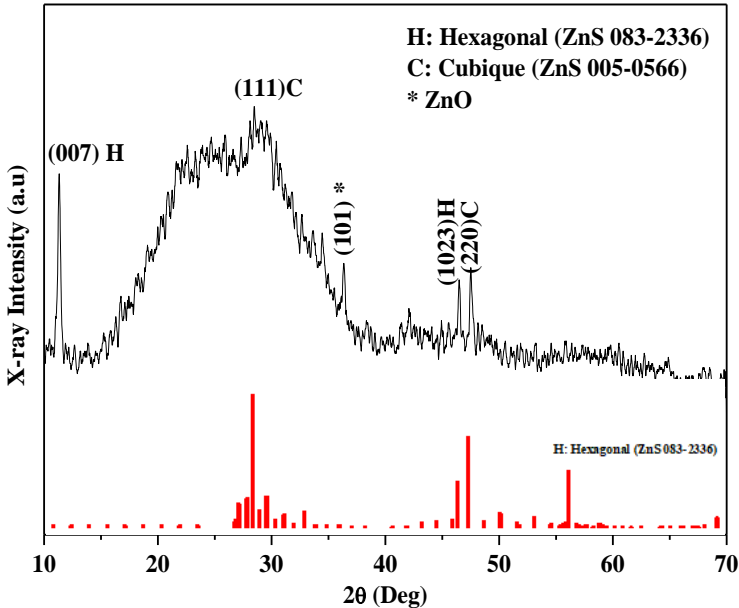

Fig.4 X-ray diffractogram of ZnS thin film synthesized by spray pyrolysis
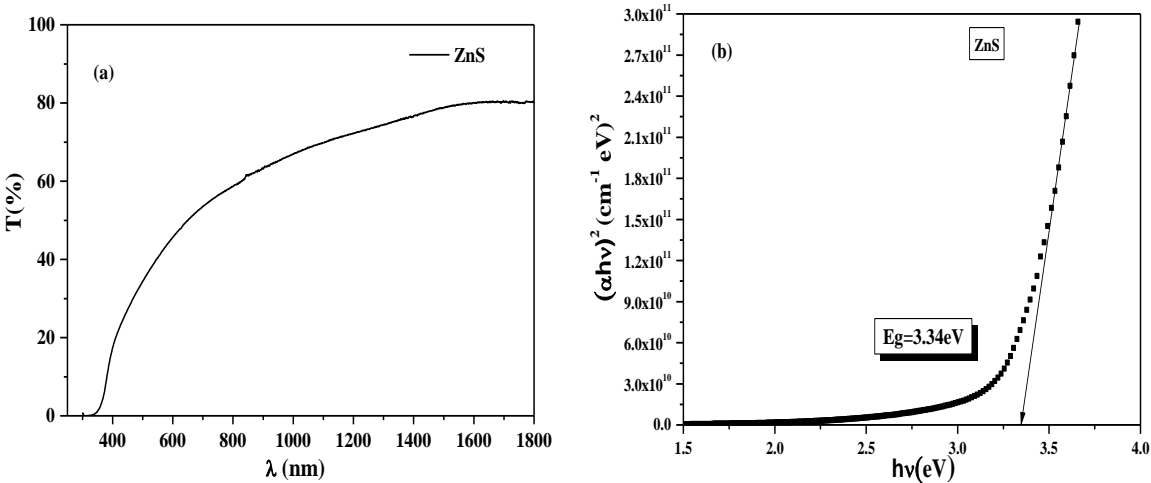

Fig.5 Optical transmittance spectrum (a) and Tauc plot of $(\alpha h\nu)^2$ versus photon energy ($h\nu$) (b) of ZnS thin films.

CZTS absorbing layer properties

Fig.6 shows the X-ray diffractogram of Cu_2ZnSnS_4 (CZTS) thin films deposited by spray sandwich technique on glass substrate. It can be seen three diffraction peaks at 2θ= 28.52°, 47.53° and 56.38° which are attributed to the kesterite Cu_2ZnSnS_4 thin films (JCPDS00-026-0575), space group I-42m. The three peaks correspond to the (112), (220) and (312) planes of Cu_2ZnSnS_4 structure, respectively, with the direction [112] as preferential orientation. It is noteworthy that no other peak related to any secondary phase are observed, despite rather oxidizing spray conditions, which is in agreement with the previously published structural results [25].

The optical band gap of CZTS film was calculated from the linear extrapolation plot of $(\alpha h\nu)^2$ vs $h\nu$ with the $h\nu$−axis (Fig. 7). The value is closed to 1.48 eV, which seems consistent with the ideal CZTS thin film for solar cells application. The same results have been reported by several authors [26, 27].
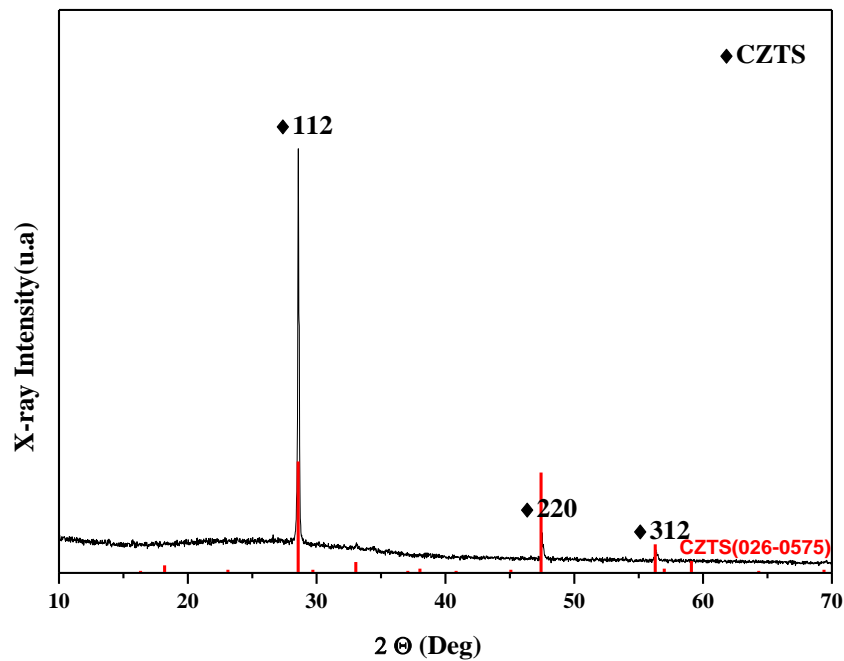

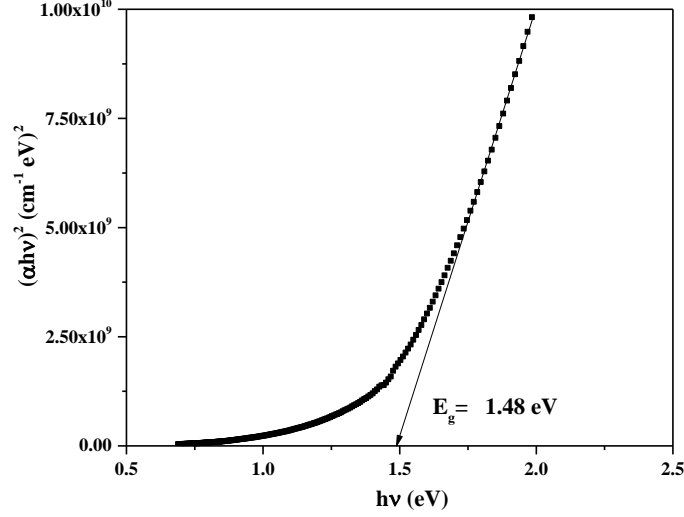Fig.6 X-ray diffractogram of CZTS thin film by spray pyrolysis

Fig. 7 Plot of $(\alpha h v)^2$ versus photon energy (hv) of CZTS thin film

Operating electronical characteristics of the solar cell devices

The metal/semiconductor heterojunctions prepared with different back contacts were investigated using the current-voltage (I-V) characteristic in the dark. The current–voltage (I-V) characteristics device yields to important information about junction parameters such as series resistance (Rs), diode ideality factor (n) and saturation current (Is).

Fig. 8 shows the current-voltage curves of the FTO/ZnS/CZTS/M, with M = Au, Ag or Pt, solar cells in the dark. It is clear that no noticeable difference between the three characteristics can be observed. All heterostructures exhibit a rectifying behavior meaning that the barrier potential formed by the contact of the metal and semiconductor is high enough to not conduct the current in both directions. Theory of thermionic emission was used to express this behaviour. According to this theory, the current is expressed by the following equation:

$$I = I_0[\exp\left(\frac{qV}{nkT}\right) - 1] \qquad \text{(Eq. 1)}$$

Where I is the measured current intensity in A, V is the applied voltage in V, I_0 is the saturation current (A), k is the Boltzmann constant (J. K^{-1}), q is the elementary electric charge (C), n is the ideality factor and T is the absolute temperature in K. The ideality factor n is given by the following equation:

$$n = \frac{q}{kT}\left(\frac{dV}{d(ln\,I)}\right) \text{(Eq. 2)}$$

The factor is determined from slope of the linear part of forward bias ln(I)–V plot. The plots of forward bias ln(I)–V characteristics of different heterojunction structure are shown in Fig. 9. According to Sah–Noyce–Shockley theory [28], the ideality factor is closed to 1 if the forward

current is dominated by the recombination in the quasi-neutral regions of the p-n junction (far from the p-n contact region), while it would be about 2 for a forward bias current dominated by the recombination in the space charge region (p-n contact region). In table 1 are reported the calculated values of the ideality factor, in addition to the series resistance and to the saturation current. As it can be seen, the ideality factors calculated in the realized heterojunctions are depending on the nature of the used metal contact. They are respectively equal to 1.6, 2.4 and 2.8 for Au, Pt and Ag contact, probably meaning that the forward bias current would be mainly controlled by the charge carrier recombination in the space charge region formed by the p-n contact which exhibits an electric field. It can be observed that the lowest value of ideality factor is obtained using Au as metal contact. This result is in agreement with that found by Boutebakh et al **[29].** They observed a similar low value of n obtained with Au back contact, as well as large value of n for the Ag and Al back contacts.

The origin of the large value of n may be due to the metal/CZTS contact. Indeed, when the contact is not ohmic, the heterojunction can be modeled as a series of diodes and resistors in series. According to Shah–Li–Schubert, the ideality factor is the sum of ideality factor of each diode. Al and Ag back contacts can be used to form Schottky contact with CZTS, contrary to Au, which can have ohmic contact with CZTS.

The series resistance Rs is very important parameter in the performance of the solar cell. Indeed, a too high series resistance considerably reduces the form factor and consequently decreases the efficiency of the cell. The series resistances were calculated from I-V curve at high bias, their values are in the order of Ω, as reported in table 1. These values can explain the obtained large ideality factor as mentioned above. The resistance series is lower when using Au as back contact. This can be due to the high work function of Au by comparison to other metals. These results are in good agreement with those found by Boutebakh et al **[29],** where they showed that the Au can be used as an alternative to Mo in CZTS-based heterojunctions.

The saturation current is obtained by extrapolating the linear part of the logarithmic plot of equation (Eq.1) to V = 0. The saturation current values for heterojunctions (Au, Pt or Ag back contact) are shown in Table 1. It is clear that the heterojunction prepared with Au as back contact has the lowest value. Several authors report that the open circuit voltage in a solar cell is better with a low saturation current.
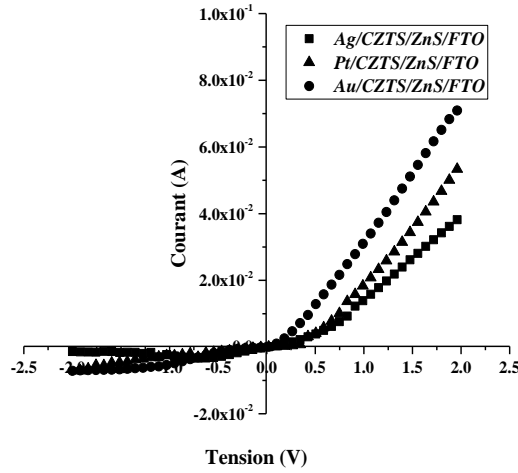
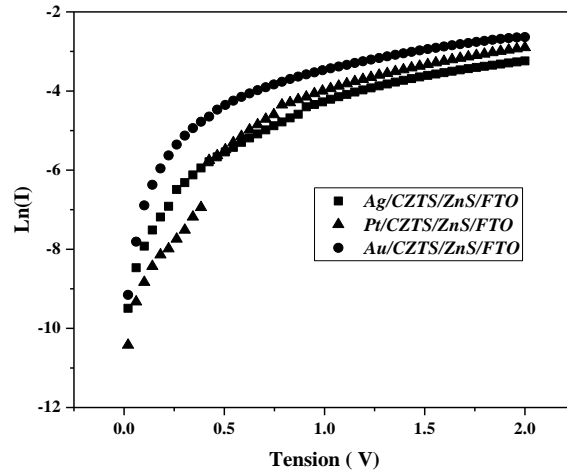Fig.8 I-V characteristics of different CZTS/ZnS heterojunctions prepared with different back contact metals.

Fig.9c Ln(I)-V plot of heterojunctions with different metal contact

Table.1 Electrical parameters of heterojunctions prepared with different metal back contact measured in dark: n ideality factor, I_0 saturation current and Rs series resistance.

Heterojunction structure	Ideality factor n	Series resistance R_s (Ω)	Saturation current $I_0 (10^{-5} A)$
Ag/CZTS/ZnS/FTO	2.8	39	11
Pt/CZTS/ZnS/FTO	2.4	29	9.5
Au/CZTS/ZnS/FTO	1.6	25	6.5

Conclusion

In this study, CZTS/ZnS based heterojunctions were produced by thermal spray pyrolysis technique. Three different back metal contact (Pt, Au and Ag) were deposited on the absorbing

layer by magnetron sputtering. Three different solar cells according to the metal nature of the back contact were tested to investigate its influence on the device electronic properties in order to find an alternative of the commonly used Molybdenum.

The devices electronical characterization exhibits a rectifying behavior. The electrical parameters prove that the Au metal can be efficiently used as back contact for CZTS based heterojunction solar cells as an alternative to Mo.

References

[1] T. K. Todorov, J. Tang, S. Bag, O. Gunawan, T. Gokmen, Y. Zhu, D.B. Mitzi, Beyond 11% Efficiency: Characteristics of State-of-the-Art Cu 2 ZnSn(S,Se) 4 Solar Cells Advanced Energy Materials **3** (2013) 34-38.

https://doi.org/10.1002/aenm.201200348

[2] W. Wang, M.T. Winkler, O. Gunawan, T. Gokmen, T.K. Todorov, Y. Zhu, D.B. Mitzi, Device Characteristics of CZTSSe Thin-Film Solar Cells with 12.6% Efficiency, Advanced Energy Material **4** (2014) 1301465.

https://doi.org/10.1002/aenm.201301465

[3] Ahmed Ziti, Bouchaib Hartiti, Hicham Labrim, Salah Fadili, Abderraouf Ridah, Bouchra Belhorma, Mounia Tahri, Study of kesterite CZTS thin films deposited by spin coating technique for photovoltaic applications, Philippe Thevenin, Superlattices and Microstructures **127** (2019) 191-200.

https://doi.org/10.1016/j.spmi.2017.11.023

[4] A. Ashfaq, J. Jacob, N. Bano, M. A. Un Nabi, A. Ali, W. Ahmad, K. Mahmood, M. 400 I. Arshad, S. Ikram, U. Rehman, N. Amin, S. Hussain, Ceramics International **45** (2019) 401 10876.

[5] Y. Wang , X.Fu , T. Wang , F. Li , D. Li , Y. Yang , X. Dong, Polyoxometalate electron acceptor incorporated improved properties of Cu2ZnSnS4-based room temperature NO2 gas sensor, Sensors and Actuators: B. Chemical, 348(2021)130683.

https://doi.org/10.1016/j.snb.2021.130683

[6] K. V. Gurav, S. W. Shin , U. M. Patil , P. R. Deshmukh, M. P. Suryawanshi, G. L. Agawane , S. M. Pawar , P. S. Patil , J. Y. Lee , C. D. Lokhande, J.H.Kim, Cu2ZnSnS4 (CZTS)-based

room temperature liquefied petroleum gas (LPG) sensor, Sensors and Actuators B: Chemical, 190 (2014) 408-413.

https://doi.org/10.1016/j.snb.2013.08.064

[7] M. Sampath, K. Sankarasubramanian, J. Archana, Y. Hayakawa, K. Ramamurthi, K. Sethuraman, Structural, optical and photocatalytic properties of spray deposited Cu2ZnSnS4 thin films with various S/(Cu+Zn+Sn) ratio, Materials Science in Semiconductor Processing, 87 (2018) 54–64.

https://doi.org/10.1016/j.mssp.2018.07.001

[8] T. Washio, T. Shinji, S. Tajima, T. Fukano, T. Motohiro, K. Jimbo, H. Katagiri, 6% Efficiency Cu2ZnSnS4-based thin film solar cells using oxide precursors by open atmosphere type CVD, Journal of Materials Chemistry **22** (2012) 4021.

https://doi.org/10.1039/C2JM16454J

[9] Z. Zhou, Y. Wang, D. Xu,Y. Zhang, Fabrication of Cu2ZnSnS4 screen printed layers for solar cells; Solar Energy Materials and Solar cells **94** (2010) 2042–2045.

https://doi.org/10.1016/j.solmat.2010.06.010

[10] R. Murugesan, S. Sivakumar, K. Karthik, P. Anandan, M. Haris, Effect of Mg/Co on the properties of CdS thin films deposited by spray pyrolysis technique, Current Applied Physics **19** (2019) 1136–1144.

https://doi.org/10.1016/j.cap.2019.07.008

11] R. Klenk, A. Steigert, T. Rissom, D. Greiner, C.A. Kaufmann, T. Unold, M.C. Lux- Steiner, Junction formation by Zn(O,S) sputtering yields CIGSebased cells with efficiencies exceeding 18%, Progress in Photovoltaics: Research and Applications **22** (2014) 161.

https://doi.org/10.1002/pip.2445

[12] J-H. Wi, T. G. Kim, J. W. Kim, W-J. Lee, D-H. Cho, W. S. Han, Y-D. Chung, Photovoltaic Performance and Interface Behaviors of Cu(In,Ga)Se2 Solar Cells with a SputteredZn(O,S) Buffer Layer by High Temperature Annealing , ACS Applied Materials & Interfaces **7** (2015) 17425.

https://doi.org/10.1021/acsami.5b04815

[13] A. M. Al-Diabat, N. M. Ahmed, M. R. Hashim, M. A. Almessiere, Growth of ZnS Thin Films using Chemical Spray Pyrolysis Technique, Materials Today: Proceedings **17** (2019) 912–920.

https://doi.org/10.1016/j.matpr.2019.06.390

[14] J. J. Scragg, J. T. W€atjen, M. Edoff, T. Ericson, T. Kubart, and C. Platzer-Bj€orkman, A Detrimental Reaction at the Molybdenum Back Contact in Cu2ZnSn(S,Se)4 Thin-Film Solar Cells, J. Am. Chem. Soc. 134, 19330–19333 (2012).

https://doi.org/10.1021/ja308862n

[15] M. Patel, A. Ray, Enhancement of output performance of Cu2ZnSnS4 thin film solar cells— A numerical simulation approach and comparison to experiments, Physica B **407** (2012) 4391–4397.

https://doi.org/10.1016/j.physb.2012.07.042

[16] WTheiss Hardware and software for optical spectroscopy, http://www.mtheiss.com/.

[17] E. Mokaripoor, M. M. Bagheri-Mohagheghi, Study of structural, electrical and photoconductive properties of F and P co-doped SnO2 transparent semiconducting thin film deposited by spray pyrolysis, Materials Science in Semiconductor Processing **30** (2015) 400.

https://doi.org/10.1016/j.mssp.2014.10.049

[18] F. El Akkad, T. A. P. Paulose, Optical transitions and point defects in F:SnO2 films: Effect of annealing, Applied Surface Science **295** (2014) 8.

https://doi.org/10.1016/j.apsusc.2013.12.057

[19] R. Thomas, T. Mathavan, Mohd**.** Shkir, S. AlFaify, Hyun-Seok Kim, A. Kathalingam,Materials, Influence of yttrium doping on microstructural and optical properties of FTO thin films prepared by nebulizer spray technique,Today Communications **24** (2020) 101087.

https://doi.org/10.1016/j.mtcomm.2020.101087

[20] R. Swapna, T. Srinivasa Reddy, K. Venkateswarlu, M.C.S. Kumar, Effect of Post-Annealing on the Properties of Eu Doped ZnO Nano Thin Films, Procedia Materials Science **10** (2015) 723–729.

10.1016/j.mspro.2015.06.085

[21] F. Long, W. M. Wang, Z. K. Cui, L. Z. Fan, Z. Zou, T.K. Ji, An improved method for chemical bath deposition of ZnS thin films, Chemical Physics Letters **462** (2008) 84.

https://doi.org/10.1016/j.cplett.2008.07.064

[22] K. G. Deepa, M. Sunil Anantha, Jampana Nagaraju, Highly transparent ZnS buffer layer prepared by ultrasonic spray pyrolysis for photovoltaic applications, Journal of Analytical and Applied Pyrolysis **126** (2017) 188-193.

https://doi.org/10.1016/j.jaap.2017.06.009

[23] H. Ke, S. Duo, T. Liu, Q. Sun, C. Ruan, X. Fei, J. Tan, S. Zhan, Effect of temperature on structural and optical properties of ZnS thin films by chemical bath deposition without stirring the reaction bath, Materials Science in Semiconductor Processing **18** (2014) 28-35.

https://doi.org/10.1016/j.mssp.2013.10.022

[24] S. Mondal, S. Bhattacharyya, P. Mitra, Effect of Al doping on microstructure and optical band gap of ZnO thin film synthesized by successive ion layer adsorption and reaction, Pramana **80** (2013) 315-326.

DOI: 10.1007/s12043-012-0463-6

[25] Kheraj, V., Patel, K.K., Patel, S.J., Shah, D.V., 2013. Synthesis and characterisation ofCopper Zinc Tin Sulphide (CZTS) compound for absorber material in solar-cells. J.Cryst. Growth. 362, 174–177.

https://doi.org/10.1016/j.jcrysgro.2011.10.034.

[26] J. Tauc, Amorphous and Liquid Semiconductors Plenium Press (1974), New York.

http://dx.doi.org/10.1007/978-1-4615-8705-7

[27] D. Miao, J. Xu, S. Jiang, X. Ning, J. Liu, S. Shang, Crystallization temperature investigation of Cu2ZnSnS4 by using Differential scanning calorimetry (DSC), Ceramics International **44** (2018) 4256–4261.

10.1016/j.ceramint.2017.12.006

[28] C. Sah, R. N. Noyce, W. Shockley, Carrier Generation and Recombination in P-N Junctions and P-N Junction Characteristics, Proceedings of the IRE (1957) 1228.

10.1109/JRPROC.1957.278528

[29] F. Z. Boutebakh, M. Lamri Zeggar, N. Attaf, M. S. Aida, Electrical properties and back contact study of CZTS/ZnS heterojunction, Optik **144** (2017) 180-190

doi:10.1016/j.ijleo.2017.06.080